Eur. Phys. J. C 14, 165–178 (2000)
Digital Object Identifier (DOI) 10.1007/s100520000332

THE EUROPEAN PHYSICAL JOURNAL C

Search and identification of scalar and vector leptoquarks at HERA with polarization

P. Taxil[1,2], E. Tuğcu[1,2,3], J.-M. Virey[1,2,4,a]

[1] Centre de Physique Théorique[b], CNRS-Luminy, Case 907, 13288 Marseille Cedex 9, France
[2] Université de Provence, Marseille, France
[3] Galatasaray University, Çırağan Cad. 102, Ortaköy 80840-İstanbul, Turkey
[4] Institut für Physik, Universität Dortmund, 44221 Dortmund, Germany

Received: 9 December 1999 / Published online: 17 March 2000 – © Springer-Verlag 2000

Abstract. We analyze the effects of scalar and vector leptoquarks on various observables in electron (positron)–proton deep inelastic scattering. In view of the future program of the HERA collider, with a high luminosity and also with polarization, we present the constraints that can be reached using this facility for several leptoquark scenarios. We address the question of the identification of the nature of a leptoquark when it is discovered. We emphasize the relevance of having polarized lepton and proton beams in order to completely disentangle the various leptoquark models. This study is also relevant in the context of the TESLA×HERA project.

1 Introduction

Many extensions of the standard model (SM), like for instance supersymmetry (SUSY) or grand unified theories (GUTs), predict the existence of leptoquarks (LQs), which are particles that couple directly to quark–lepton pairs. In general there is no particular prediction for the masses of these LQs, which can range from the electroweak (EW) scale to the GUT scale. However, an interesting possibility is the case of SUSY models where the $R_{\rm Parity}$ symmetry [1] is violated (for a recent review on this subject see [2]). Then some $\not{R}_p$-squarks have direct couplings to electron–quark pairs and are completely analogous to some of the LQs considered here. The equivalence between $\not{R}_p$-squarks and LQs is described, for instance, in [3]. An interesting feature of the SUSY models with $\not{R}_p$-squarks is that the squarks could have some relatively low masses (between the EW and the TeV scales) since SUSY is believed to be broken at the TeV scale.

In this paper we will not consider any precise $\not{R}_p$ - squarks model but we rather adopt the "model independent" approach of Buchmüller–Rückl–Wyler (BRW) [4], where the LQs are classified according to their quantum numbers and have to fulfil several assumptions like B and L conservation (to avoid rapid proton decay) and $SU(3)\times SU(2)\times U(1)$ invariance. We refer to [4] for more details. The interaction lagrangian for scalar leptoquarks is given by

$$\begin{aligned}\mathcal{L}_{\rm scal} = &\left(g_{1\rm L}\bar{q}^c_{\rm L}{\rm i}\tau_2\ell_{\rm L} + g_{1\rm R}\bar{u}^c_{\rm R}e_{\rm R}\right)\cdot\mathbf{S_1} + \tilde{g}_{1\rm R}\bar{d}^c_{\rm R}e_{\rm R}\cdot\tilde{\mathbf{S}}_{\mathbf{1}}\\ &+ g_{3\rm L}\bar{q}^c_{\rm L}{\rm i}\tau_2\tau\ell_{\rm L}\cdot\mathbf{S_3}, + \left(h_{2\rm L}\bar{u}_{\rm R}\ell_{\rm L} + h_{2\rm R}\bar{q}_{\rm L}{\rm i}\tau_2 e_{\rm R}\right)\cdot\mathbf{R_2}\\ &+ \tilde{h}_{2\rm L}\bar{d}_{\rm R}\ell_{\rm L}\cdot\tilde{\mathbf{R}}_{\mathbf{2}},\end{aligned} \tag{1}$$

where the scalar LQs S_1, $\tilde{S}_1$ are singlets and S_3 is a triplet, all with fermionic number $(F = 3B + L)$ $F = 2$. R_2 and $\tilde{R}_2$ are doublets with $F = 0$. $\ell_{\rm L}$, $q_{\rm L}$ ($e_{\rm R}$, $d_{\rm R}$, $u_{\rm R}$) are the usual lepton and quark doublets (singlets). For vector LQs the lagrangian is

$$\begin{aligned}\mathcal{L}_{\rm vect} = &\left(h_{1\rm L}\bar{q}_{\rm L}\gamma^\mu\ell_{\rm L} + h_{1\rm R}\bar{d}_{\rm R}\gamma^\mu e_{\rm R}\right)\cdot\mathbf{U}_{\mathbf{1}\mu}\\ &+ \tilde{h}_{1\rm R}\bar{u}_{\rm R}\gamma^\mu e_{\rm R}\cdot\tilde{\mathbf{U}}_{\mathbf{1}\mu}\\ &+ h_{3\rm L}\bar{q}_{\rm L}\tau\gamma^\mu\ell_{\rm L}\cdot\mathbf{U}_{\mathbf{3}\mu}\\ &+ \left(g_{2\rm L}\bar{d}^c_{\rm R}\gamma^\mu\ell_{\rm L} + g_{2\rm R}\bar{q}^c_{\rm L}\gamma^\mu e_{\rm R}\right)\cdot\mathbf{V}_{\mathbf{2}\mu}\\ &+ \tilde{g}_{2\rm L}\bar{u}^c_{\rm R}\gamma^\mu\ell_{\rm L}\cdot\tilde{\mathbf{V}}_{\mathbf{2}\mu},\end{aligned} \tag{2}$$

where the vector $U_{1\mu}$, $\tilde{U}_{1\mu}$ are singlets and $U_{3\mu}$ is a triplet, all with $F = 0$, and $V_{2\mu}$, $\tilde{V}_{2\mu}$ are doublets with $F = 2$.

Therefore, if one takes into account the left- and right-handed chiralities $\mathcal{L}_{\rm scal}+\mathcal{L}_{\rm vect}$ yields 14 independent models of LQs. From these two lagrangians one can deduce some properties of the LQ models which are compiled in Table 1 of [3]. A point which is important to notice is that the LQ couplings are flavor dependent. In what follows we generically denote by λ any LQ coupling and by M the associated mass.

[a] Fellow of the "Alexander von Humboldt" Foundation; present address: Centre de Physique Théorique[b], CNRS-Luminy, Case 907, 13288 Marseille Cedex 9, France;
e-mail: virey@cpt.univ-mrs.fr
[b] Unité Propre de Recherche 7061

In addition, in order to simplify the analysis, we make the following assumptions:

(i) the LQ couples to the first generation only,
(ii) one LQ multiplet is present at a time,
(iii) the different LQ components within one LQ multiplet are mass degenerate,
(iv) there is no mixing among LQs.

The LQs are severely constrained by several different experiments, and we refer to [5–7] for some detailed discussions. Here we only quote the most important facts.

(1) Leptonic pion decays and $(g-2)_\mu$ measurements indicate that the LQs must be chiral [5,6] (e.g. S_1 and R_2 could have left-handed or right-handed couplings but not both).
(2) To avoid the stringent constraints from FCNC processes the simplest assumption is to impose "family diagonal" couplings for the LQs, namely they couple to only one generation [5].
(3) There are some collider constraints coming from Tevatron through the searches for LQ pair production. This process, which involves the color properties of the LQs, yields some bounds on the mass of the LQs independently of the λ coupling and of the particular scalar or vector LQ model. However, these mass bounds are strongly dependent on the branching ratio $BR(LQ \to eq)$, and the values quoted below correspond to the maximal case $BR = 1$.
For the scalar LQ models, the CDF and D0 collaborations at the Tevatron have combined their data to provide [8] the constraint: $M > 242\,\mathrm{GeV}$ $(BR = 1)$. The dependence of these limits on BR is presented in [8]. For the vector LQ models the situation is more complex since, in general, the experimental bounds depend on two new parameters: κ_g and λ_g. These two parameters correspond to the possible anomalous couplings present at vertices involving gluon(s) plus vector LQ(s) [9]. The value of the cross sections depends on these two parameters. In particular, the smallest cross sections do not correspond in general to the ones obtained for "pure" gauge boson couplings (i.e. $\kappa_g = 0$, $\lambda_g = 0$).
The D0 collaboration has published some mass bounds for vector LQs for several values of (κ_g,λ_g) [10]. They obtained $M > 340\,\mathrm{GeV}$ $(BR = 1)$ for $(\kappa_g = 0,\lambda_g = 0)$, but the weakest constraint, corresponding to the minimal cross section, $M > 245\,\mathrm{GeV}$ $(BR = 1)$ is obtained for $(\kappa_g = 1.3,\ \lambda_g = -0.2)$.
To conclude this part, we remark that the minimal mass bound for vector LQs is close to the mass bound for scalar LQs, and we recall that these bounds are strongly dependent on BR. For instance, the $R\!\!\!/_p$ - squarks models mentioned above are not coupled to $e-q$ pairs only, but also to some superpartners (R_p-conserving decays) which means that $BR < 1$. As a consequence, for some particular models, BR can be relatively small, giving much lower LQs mass limits.
(4) Low energy neutral current data, in particular from atomic parity violation on cesium atoms (APV) experiments, give in general the strongest bounds on the ratio M/λ. In fact, the last experimental results on the measurements of $Q_W(\mathrm{Cs})$, the weak charge for cesium atoms, give [11] $Q_W^{\mathrm{exp}} = -72.06 \pm (0.28)_{\mathrm{exp}} \pm (0.34)_{\mathrm{th}}$. For the SM we expect [12] $Q_W^{\mathrm{th}} = -72.84 \pm 0.13$. This means that the SM is excluded at the 1.8σ level. However this discrepancy is not huge and even if the experimental errors have strongly decreased compared with the preceding experiments, they are still sizable. Thus we take these results with some caution.
Nevertheless, we have used the formula from [6] to compute the constraints on the LQ models taking these new data into account.
In fact, since the Q_W experimental value does not exactly correspond to the SM prediction, we need some new physics effects to fit the data. Consequently, on the one hand, if a particular LQ model gives a deviation for Q_W which is in the wrong direction with respect with the measured value, then it is simply excluded for any value of M/λ. On the other hand, if the deviation of the LQ model is in the right direction, this LQ model helps to fit the data and we get not only an upper bound for M/λ but a window of "presence", namely the LQ should have a ratio M/λ in this window to give agreement between data and theory. The figures we obtain for the BRW LQ models considered here are given in Table 1.
In this table a cross indicates that the model is excluded.
Note that similar bounds have been obtained for LQ models from the GUT group E_6 [13]. These constraints can be relaxed if there are some compensating contributions coming from more than one source of new physics [14]. Adopting a conservative attitude we do not consider the last measurement of Q_W as clear evidence for new physics, and in the following we will consider that *all* the LQ models can still exist at low energy scales and can induce some effects in deep inelastic scattering (DIS).
(5) Finally, there are also some collider constraints coming from LEP [15] and HERA [16]. In fact, depending on the particular LQ model involved the limits obtained at these facilities cover in general a small part of the parameter space (M,λ).
The analysis of LQ effects at present or future ep machines is of particular relevance since such particles

Table 1. Limits on M/λ in GeV at 95% CL from APV

Leptoquark	Limits	Leptoquark	Limits
$S_{1\mathrm{L}}$	1600–3900	$U_{1\mathrm{L}}$	×
$S_{1\mathrm{R}}$	×	$U_{1\mathrm{R}}$	2400–5800
$\tilde{S}_{1\mathrm{R}}$	×	$\tilde{U}_{1\mathrm{R}}$	2300–5500
$S_{3\mathrm{L}}$	2900–7000	$U_{3\mathrm{L}}$	×
$R_{2\mathrm{L}}$	×	$V_{2\mathrm{L}}$	2400–5800
$R_{2\mathrm{R}}$	2350–5650	$V_{2\mathrm{R}}$	×
$\tilde{R}_{2\mathrm{L}}$	×	$\tilde{V}_{2\mathrm{L}}$	2300–5500

could be produced in the s-channel [4]. In this paper, we complete and extend the analysis which has been presented recently [17] on the effects of scalar LQs in the neutral current (NC) and charged current (CC) channels at HERA.

We will concentrate on the HERA collider with high integrated luminosities and also with a slightly higher energy in the center of mass. Namely, we take $s^{1/2} = 380\,\mathrm{GeV}$ in order to increase the domain of sensitivity for the LQ models. This value for the energy could be reached in the future at HERA [18]. However, we consider also the case $s^{1/2} = 300\,\mathrm{GeV}$ in order to test the impact of the energy value on the capabilities of the HERA collider to discover LQs. In addition, we are also concerned with a possible new ep collider running at much higher energies $s^{1/2} = 1\,\mathrm{TeV}$, like the TESLA×HERA project [19].

An other important point of our analysis is that we consider the case where polarized beams are available. Indeed, thanks to the progress which have been performed by the RHIC Spin Collaboration [20] at Brookhaven, the acceleration of polarized proton beams up to high energies is becoming a real possibility. Adding this opportunity to the fact that high intensity polarized lepton beams will certainly be available soon at HERA, and also at a future linear accelerator, some new windows could be opened with $\vec{e}\vec{p}$ collisions. The resulting potentialities for HERA physics have been discussed in several recent workshops [21–24].

This paper is organized as follows. In Sect. 2, we estimate the constraints on the parameter space that can be reached in the future at HERA for several leptoquark scenarios and we compare these results with the present bounds. In Sect. 3, we propose a strategy for the identification of the various LQ models. In particular, we show that both electron and proton polarizations ($\vec{e} + \vec{p}$) are necessary to disentangle the different models. Finally, we summarize our results and we draw our conclusions in Sect. 4. The details of the formulas we have used are given in the Appendix.

2 Discovery limits from future ep experiments

We consider the HERA collider with e^- or e^+ beams but with some high integrated luminosities, namely $L_{e^-} = L_{e^+} = 500\,\mathrm{pb}^{-1}$. The other parameters for the analysis being : $s^{1/2} = 380\,\mathrm{GeV}$, $0.01 < y < 0.9$, $(\Delta\sigma/\sigma)_{\mathrm{syst}} = 2\%$ and we use the GRV partonic distribution functions (pdf) set [25].

We present in Fig. 1 the discovery limits at 95% CL for the various LQ models that we obtain from a χ^2 analysis performed on the unpolarized NC cross sections $\mathrm{d}\sigma/\mathrm{d}Q^2$ for $ep \to eX$ at leading order (see the Appendix).

Next-to-leading order (NLO) QCD corrections to the production cross section have been estimated recently [26, 27]. In the mass range we consider, K-factors increase the cross section by up to 30–50% according to two different calculations [26, 27]. This means that our bounds are somewhat pessimistic. On the other hand, we expect that the asymmetries we will present later will be less affected by NLO corrections since K-factors should cancel in the ratios.

From these plots we see that there are clearly two different domains of constraints in the (M, λ) plane. In the "real domain" ($M < 380\,\mathrm{GeV}$) production in the s-channel is by far dominant due to the resonance. The "virtual domain" for masses above 380 GeV corresponds to the production or exchange of an off-shell LQ and the SM cross section is less affected. As a consequence the bounds are weaker. In addition we see on this figure that the LQs which couple preferentially to d-quarks ($\tilde{S}_1$, $\tilde{R}_2$) and ($V_{2\mathrm{L}}$,$U_{1\mathrm{R}}$) are less constrained compared to the others, since u-quarks are dominant in the proton. Isospin symmetry implies that we would need en collisions (with the same values for $s^{1/2}$ and L) to constrain these two LQs at the same level.

Besides the discovery bounds obtained from the unpolarized NC cross sections, it is interesting to examine which sensitivity could be obtained from other observables like the unpolarized CC cross sections, the single or double polarized cross sections (in NC or CC processes) or some spin asymmetries.

Charged current cross sections

Concerning the CC channel, in DIS the SM process corresponds to W exchanges: $ep \to \nu X$. The LQs which have both couplings to eq and $e\nu$ pairs should also induce some effects in CC processes. Note that within our assumptions (no mixing) only $S_{1\mathrm{L}}$, S_3, $U_{1\mathrm{L}}$ and U_3 could induce some effects in the CC sector.

The effects in CC at HERA have been analyzed some time ago in [28] in the framework of some specific models based on superstring-inspired E_6. More recently they were considered again, essentially in the context of the so-called HERA anomaly problem (for a review and references, see [29]). Then, the CC process was considered to analyze the origin of the LQ rather than with the purpose of discovery. Here we can confirm this strategy since our χ^2 analysis shows that the sensitivity of the CC unpolarized cross section to the presence of the LQs is well below the one of the NC unpolarized cross section. Therefore, in the following of this section we do not consider anymore the CC processes.

Polarized cross sections

When polarized beams are available, the basic observables are the helicity dependent (= polarized) cross sections. Polarization adds several types of systematic errors to the unpolarized case (see [30] for example). Then, in general, with polarized beams one prefers to use some spin asymmetries rather than the individual polarized cross sections. Indeed, most of the systematics cancel in the differences between the cross sections in various helicity states (numerator) and also in the ratio. However, at HERA, one

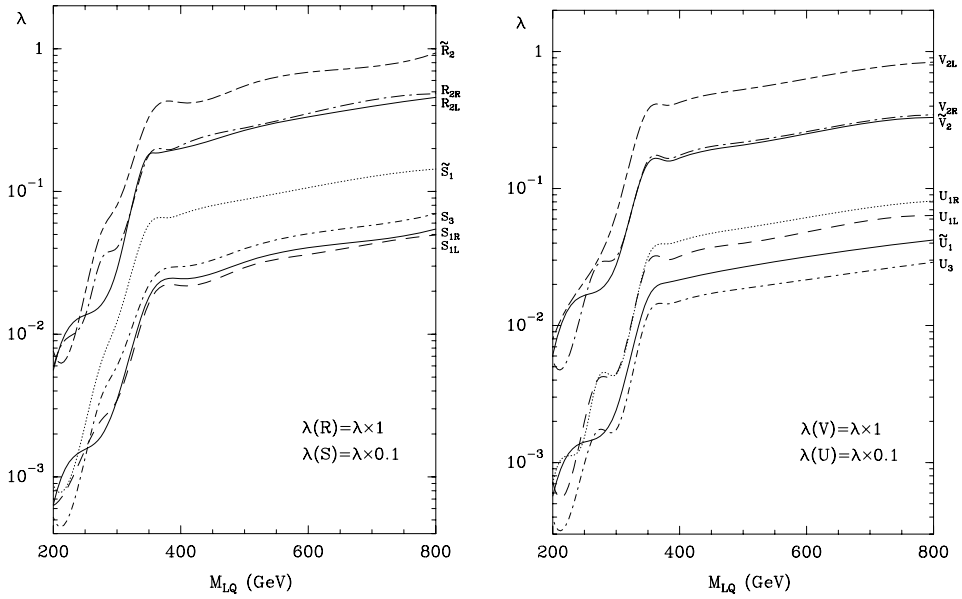

Fig. 1. Discovery limits at 95% CL for the various LQ models at HERA

can expect relatively small systematics for the polarized cross sections themselves. In particular, one expects [31]

$$\left(\frac{\Delta\sigma^{h_e}}{\sigma^{h_e}}\right)_{\text{syst}} = 2\text{–}5\% \tag{3}$$

and

$$\left(\frac{\Delta\sigma^{h_e,h_p}}{\sigma^{h_e,h_p}}\right)_{\text{syst}} = 5\text{–}10\%, \tag{4}$$

where h_e, h_p are the helicities of the electron and of the proton (protons are not polarized in the first case).

Therefore, we have computed the sensitivities of the polarized cross sections using the most favorable values for the systematics. For the calculations we have assumed a degree of polarization of $P = 70\%$ and used the GRSV polarized pdf set [32].

In comparison with the unpolarized NC cross sections we find, on the one hand, that the double polarized NC cross sections have a sensitivity of the same order and, on the other hand, that the single polarized NC cross sections have a slightly better sensitivity by roughly 2–10% (the precise value depending on the model). These conclusions are only indicative because the sensitivity of the cross sections (polarized or not) are strongly dependent on the systematics.

Spin asymmetries

Finally, we have also computed the constraints that can be reached by studying some parity violating (PV) spin asymmetries (definitions below). Concerning the systematic errors, we have considered $(\Delta A/A)_{\text{syst}} = 10\%$ which is the expected value [30]. It appears that when both lepton and proton beams are polarized, the limits are very close to the ones obtained in the unpolarized case. When lepton polarization only is available the bounds are slightly weaker.

In conclusion, for the purpose of discovery the most simple way to proceed at HERA is to consider the NC unpolarized cross sections.

In Fig. 2 we present a comparison in the (M, λ) plane between the present constraints and what could be achieved in the future in *ep* collisions.

We have shown the cases of two different scalars and two different vectors for illustration. The situation is very similar for the ten remaining models. For future experiments one considers, on the one hand, the HERA collider with a higher energy of $s^{1/2} = 380$ GeV but also with $s^{1/2} = 300$ GeV and, on the other hand, the very interesting project TESLA(e)×HERA(p) where an energy of $s^{1/2} = 1\,\text{TeV}$ could be reached [19]. The integrated luminosities are $L_{e^-} = L_{e^+} = 500\,\text{pb}^{-1}$ in all cases.

We can remark the following:

(1) For most of the models, LEP limits are already covered by the present HERA data [16].
(2) Concerning the constraints from APV experiments, we show the allowed windows which are obtained by taking seriously into account the recent results on Q_W and their interpretation in terms of new physics due to a LQ. Then, in the virtual domain, the expected sensitivity of the future HERA program would not give better insights than the APV experiments with their present sensitivity. In the real domain the situation is different.
(3) Tevatron data cover an important part of the parameter space in the real domain. However, we recall that the bounds obtained from LQ pair production at Tevatron are strongly sensitive to $BR(LQ \to eq)$. This is the case for R-parity-violating squarks in SUSY models [3].
(4) To increase the window of sensitivity in the real domain, it is more important to increase the energy than the integrated luminosity.

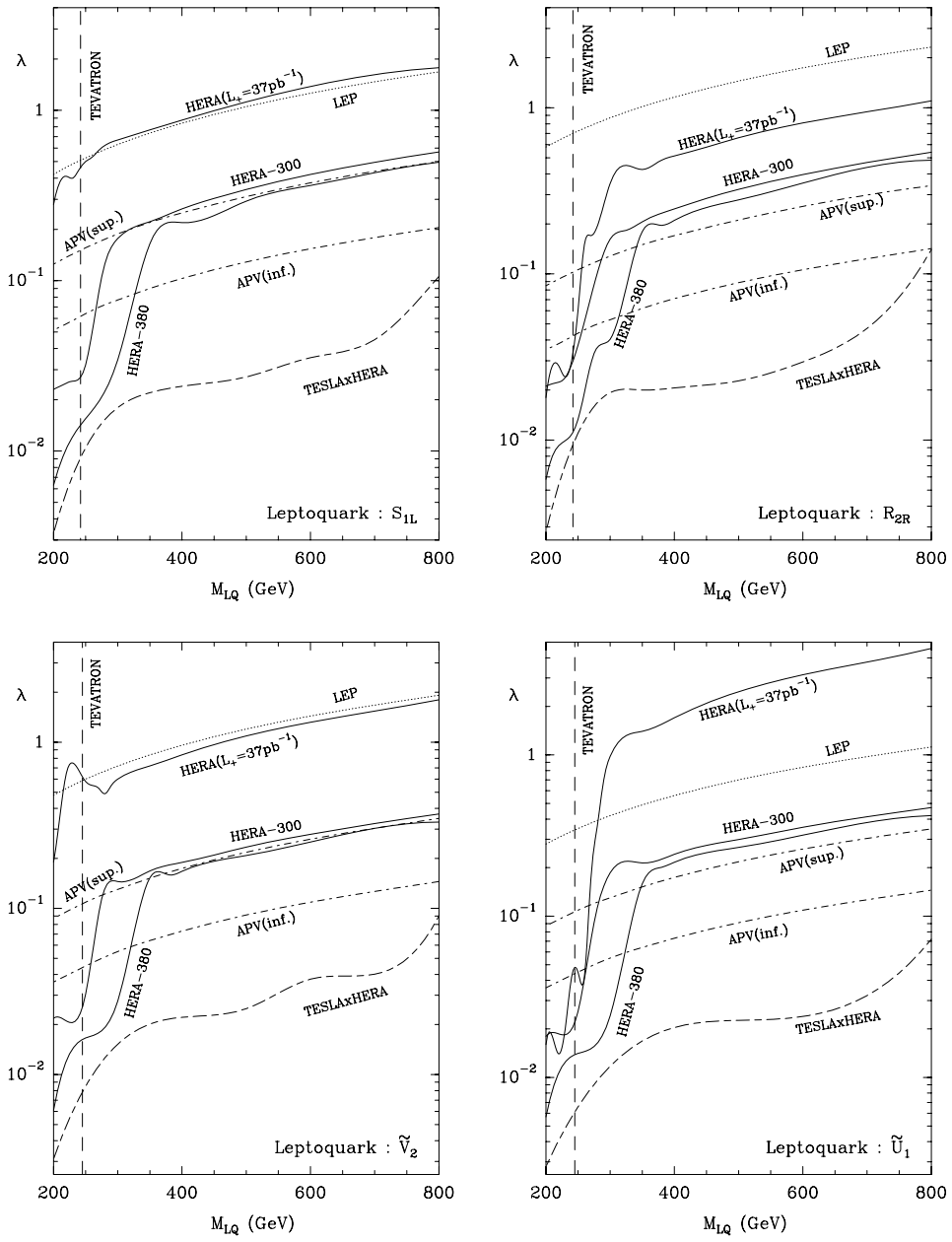

Fig. 2. Constraints at 95% CL for various present and future experiments for $R_{2\mathrm{R}}$, $S_{1\mathrm{L}}$, $\tilde{V}_2$ and $\tilde{U}_1$

(5) The TESLA×HERA project will give access to a domain (both real and virtual) which is unconstrained presently. However, if this project is achieved, it will run at a time where the LHC will be running too. Then there will be some important constraints on M from LQ pair production at LHC, but again those constraints will be strongly model dependent i.e. BR dependent.

We conclude that there are still some windows for discovery at HERA and at future *ep* machines, in complementarity with the constraints coming from LQ pair production at pure hadronic colliders. We now turn to the problem of the identification of the nature of the LQ, a problem which is much more difficult and where polarization will be of great help.

3 Strategy for the identification of the various LQ models

3.1 Observables in a future HERA program

Besides the unpolarized differential cross sections $\mathrm{d}\sigma_{\pm}/\mathrm{d}y$ and $\mathrm{d}\sigma_{\pm}/\mathrm{d}Q^2$ in both the e^+ and e^- channels, we have considered a large set of polarized observables like the spin asymmetries. Indeed, since the LQs are chiral one can expect that the most important effects will appear on the parity violating (PV) spin asymmetries which can be defined when both beams are polarized or when there is lepton polarization only. Parity conserving (PC) spin asymmetries will also be of great help, as well as some charge asymmetries.

We will only define and discuss below the quantities which turned out to be the best ones to pin down the nature of the LQ and which have the stronger sensitivity to this kind of new physics. We will start by recalling the definitions of the relevant asymmetries.

If one beam is polarized (in practice, the lepton beam) one can define the single-spin parity-violating longitudinal asymmetry $A_{\rm L}(e^t)$ ($t = \pm$ according to the electric charge of the lepton):

$$A_{\rm L}(e^t) = \frac{\sigma_t^- - \sigma_t^+}{\sigma_t^- + \sigma_t^+}, \tag{5}$$

where $\sigma_t^{h_e} \equiv (\mathrm{d}\sigma_t/\mathrm{d}Q^2)^{h_e}$ and h_e is the helicity of the lepton. In addition, when both lepton and proton beams are polarized, some double spin PV asymmetries can be defined [33]. For instance $A_{\rm LL}^{\rm PV}$ is defined as

$$A_{\rm LL}^{\rm PV}(e^t) = \frac{\sigma_t^{--} - \sigma_t^{++}}{\sigma_t^{--} + \sigma_t^{++}}, \tag{6}$$

where $\sigma_t^{h_e h_p} \equiv (\mathrm{d}\sigma_t/\mathrm{d}Q^2)^{h_e h_p}$, and h_e, h_p are the helicities of the lepton and the proton, respectively.

On the other hand, with longitudinally polarized beams, one needs two polarizations to define some parity-conserving (PC) asymmetries $A_{\rm LL}^{\rm PC}$. These well-known quantities have been extensively used in polarized DIS to determine the spin structure of the nucleon [34]. Here we will use

$$A_1^{\rm PC} = \frac{\sigma_-^{--} - \sigma_-^{-+}}{\sigma_-^{--} + \sigma_-^{-+}}, \tag{7}$$

$$A_2^{\rm PC} = \frac{\sigma_-^{++} - \sigma_-^{+-}}{\sigma_-^{++} + \sigma_-^{+-}}, \tag{8}$$

and

$$A_3^{\rm PC} = \frac{\sigma_+^{++} - \sigma_+^{+-}}{\sigma_+^{++} + \sigma_+^{+-}}. \tag{9}$$

Finally, since e^- as well as e^+ (polarized) beams will be available at HERA, one can define a large set of (polarized) charge asymmetries [35]. Among this set, only the following turned out to be relevant for our purpose:

$$\begin{aligned} B_U &= \frac{\sigma_-^{--} - \sigma_-^{++} + \sigma_+^{++} - \sigma_+^{--} + \sigma_-^{-+} - \sigma_-^{+-} + \sigma_+^{-+} - \sigma_+^{+-}}{\sigma_-^{--} + \sigma_-^{++} + \sigma_+^{++} + \sigma_+^{--} + \sigma_-^{-+} + \sigma_-^{+-} + \sigma_+^{-+} + \sigma_+^{+-}} \\ &= \frac{\sigma_-^{-0} - \sigma_-^{+0} + \sigma_+^{0+} - \sigma_+^{0-}}{\sigma_-^{-0} + \sigma_-^{+0} + \sigma_+^{0+} + \sigma_+^{0-}}, \end{aligned} \tag{10}$$

and

$$\begin{aligned} B_V &= \frac{\sigma_-^{--} - \sigma_-^{++} + \sigma_+^{--} - \sigma_+^{++} + \sigma_-^{+-} - \sigma_-^{-+} + \sigma_+^{-+} - \sigma_+^{+-}}{\sigma_-^{--} + \sigma_-^{++} + \sigma_+^{--} + \sigma_+^{++} + \sigma_-^{+-} + \sigma_-^{-+} + \sigma_+^{-+} + \sigma_+^{+-}} \\ &= \frac{\sigma_-^{0-} - \sigma_-^{0+} + \sigma_+^{-0} - \sigma_+^{+0}}{\sigma_-^{0-} + \sigma_-^{0+} + \sigma_+^{-0} + \sigma_+^{+0}}, \end{aligned} \tag{11}$$

where the index 0 means unpolarized and the order h_e, h_p has been respected. Note that both lepton and proton polarizations are necessary if one wants to measure these quantities.

3.2 Unpolarized case

We consider first the case of neutral currents.

If a LQ is present in an accessible kinematic range at HERA, it will be discovered from the analysis of $\mathrm{d}\sigma_t/\mathrm{d}Q^2$ which have the greatest "discovery" potential. However, if one starts trying to pin down the various models, both $\mathrm{d}\sigma_t/\mathrm{d}y$ and $\mathrm{d}\sigma_t/\mathrm{d}Q^2$ have to be analyzed simultaneously.

As is well known [4] the use of e^- or e^+ beams allows the separation of the 14 models of LQs into two classes according to the value of the fermionic number F. This comes from the dominant (LQ mediated) interaction between a valence quark and an e^- ($F = 2$) or an e^+ ($F = 0$).

Hence, a deviation from $\mathrm{d}\sigma_-^{\rm SM}/\mathrm{d}Q^2$ indicates the class ($S_{\rm type}$ or $V_{\rm type}$), whereas a deviation from $\mathrm{d}\sigma_+^{\rm SM}/\mathrm{d}Q^2$ corresponds to the class ($R_{\rm type}$ or $U_{\rm type}$).

Then, the y dependence, which is obtained from the two $\mathrm{d}\sigma_t/\mathrm{d}y$, is the best way to discriminate between a scalar and a vector interaction. Indeed, the SM background displays $\mathrm{d}\sigma_t/\mathrm{d}y \sim 1/y^2$ when the pure vector LQ case goes as y and the pure scalar LQ is constant in y. It is straightforward to obtain these behaviors from the formulas given in [4,3] and in the appendix.

We illustrate this pattern in Fig. 3 for two different choices of scalar and vector LQs, with parameters allowed by the present limits. Since the separation is easy, in the following we will treat the scalar and vectors as two distinct species. Now the LQ models are separated in four distinct classes: ($S_{\rm type}$), ($R_{\rm type}$), ($V_{\rm type}$) and ($U_{\rm type}$).

On the other hand, charged current (CC) processes could in principle allow one to go further into the distinction procedure. We have seen previously that only $S_{1\rm L}$ and S_3 for scalars, and $U_{1\rm L}$ and U_3 for vectors can induce a deviation from SM expectations (if we do not assume LQs mixing[1]). This means that the analysis of $\sigma_{e^-p}^{CC}$ allows one to split the ($S_{\rm type}$) class into ($S_{1\rm L}$,S_3) and ($S_{1\rm R}$,$\tilde{S}_1$), while the ($U_{\rm type}$) class is split into ($U_{1\rm L}$,U_3) and ($U_{1\rm R}$,$\tilde{U}_1$).

In addition, it appears that when LQ exchange interferes with W exchange, $S_{1\rm L}$ and S_3 display some opposite patterns (see Appendix), and this is also the case between $U_{1\rm L}$ and U_3. However this interference term is too small to be measurable from unpolarized CC processes at HERA within the allowed parameters.

Then, if we want to go further into the identification of the LQs we need to separate "eu" from "ed" interactions, which seems to be impossible within ep collisions except if the number of anomalous events is huge [37]. If en collisions were available, the analysis of the respective ep and en production rates should allow this separation [17].

In conclusion, the ep unpolarized studies should allow the separation of the 14 LQ models into the six following classes: ($S_{1\rm L}$,S_3), ($S_{1\rm R}$,$\tilde{S}_1$), ($R_{2\rm L}$,$R_{2\rm R}$,$\tilde{R}_2$), ($U_{1\rm L}$,U_3), ($U_{1\rm R}$,$\tilde{U}_1$) and ($V_{2\rm L}$,$V_{2\rm R}$,$\tilde{V}_2$).

[1] We refer to [36] for a discussion of scalar LQs mixings.

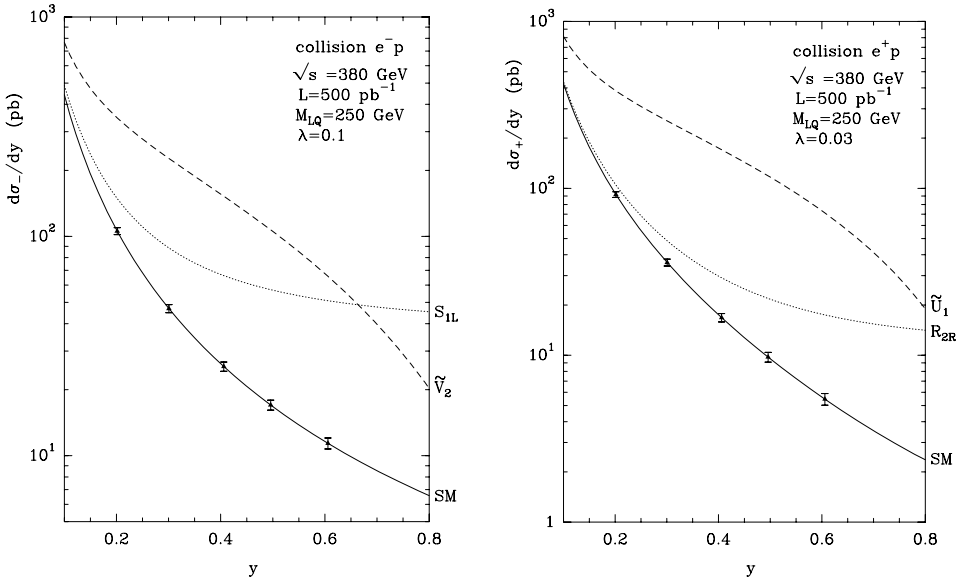

Fig. 3. $\mathrm{d}\sigma_-/\mathrm{d}y$ for $S_{1\mathrm{L}}$ and $\tilde{V}_2$, and $\mathrm{d}\sigma_+/\mathrm{d}y$ for $R_{2\mathrm{R}}$ and $\tilde{U}_1$

3.3 Polarized case

In a first step, we have tried to pin down the spin asymmetries which should allow one to disentangle the chiral structure of the new interaction. Following our previous experience [38,35] we know that the PV spin asymmetries (A_{L} or $A_{\mathrm{LL}}^{\mathrm{PV}}$) should fulfil this purpose.

Since their interactions are chiral, the LQs will induce some effects in these PV asymmetries, and the directions of the deviations from the SM expectations allow the distinction to be made between several classes of models. For instance, a positive deviation for $A_{\mathrm{L}}(e^-p)$ pins down the class ($S_{1\mathrm{L}}$,S_3) (or ($V_{2\mathrm{L}}$,$\tilde{V}_2$)) and, a negative one the class ($S_{1\mathrm{R}}$,$\tilde{S}_1$) (or $V_{2\mathrm{R}}$). Similarly, an effect for $A_{\mathrm{L}}(e^+p)$ makes a distinction between the model $R_{2\mathrm{R}}$ (or ($U_{1\mathrm{R}}$,$\tilde{U}_1$)) and the class ($R_{2\mathrm{L}}$,$\tilde{R}_2$) (or ($U_{1\mathrm{L}}$,U_3)). These properties are illustrated in Fig. 4 which displays A_{L} for e^-p and e^+p collisions with separated plots for scalar and vector LQs. The HERA and LQ parameters are given in the figure. The statistical and the 10% systematic errors are added in quadrature.

Therefore, the PV asymmetries separate the 14 BRW models into the following eight classes: ($S_{1\mathrm{L}}$,S_3), ($S_{1\mathrm{R}}$,$\tilde{S}_1$), ($R_{2\mathrm{R}}$), ($R_{2\mathrm{L}}$,$\tilde{R}_2$), ($U_{1\mathrm{L}}$,U_3), ($U_{1\mathrm{R}}$,$\tilde{U}_1$), ($V_{2\mathrm{L}}$,$\tilde{V}_2$) and ($V_{2\mathrm{R}}$). It appears that the sensitivity of the two-spin PV asymmetry $A_{\mathrm{LL}}^{\mathrm{PV}}$ is only slightly better than the one of A_{L}. Therefore, at this step, polarized protons are not mandatory.

The final step is to distinguish between an eu and an ed interaction, i.e. to obtain the flavor of the valence quark involved in the dominant interaction. With a polarized lepton beam and unpolarized protons, this flavor separation is not easy since only the different electric charges or partonic weights of u and d quarks can be used. Conversely, when polarized protons are available, it is possible to use a peculiarity of the polarized valence quark distributions, namely $\Delta u > 0$ and $\Delta d < 0$ (see e.g. [34] for a recent review). Indeed, if we pin down a spin asymmetry which is directly proportional to the Δq's, the flavor separation will be obtained from the sign of the deviation with respect with the SM value for this asymmetry. The double spin asymmetries $A_{\mathrm{LL}}^{\mathrm{PC}}$'s and the polarized charge asymmetries B_U and B_V defined above share this property. At this point we need to discuss separately the scalar case and the vector case.

Scalar case

The three $A_{\mathrm{LL}}^{\mathrm{PC}}$, A_1^{PC}, A_2^{PC}, A_3^{PC}, are the useful observables to separate the scalar LQs within the remaining classes. In Fig. 5 they are displayed for real LQ production. With the values we have chosen for the LQ parameters the separation is clear.

In fact the situation is a little bit more complex. Indeed, at this stage, we need to know if the LQ is real or virtual in order to pin down the dominant amplitude.

(1) If the LQ is on-shell, the dominant term is the squared amplitude for LQ production. This information is known from the observation of the x distribution of the events [4].
(2) If the LQ is off-shell, the dominant term is now the $\gamma \cdot LQ$ interference term. This information is known from the non-observation of the s-resonance.

The dominant term controls the behavior of the asymmetries. Since it depends on the mass of the LQ, we deduce that the behavior of the asymmetries may also be M dependent. In fact we should have a change of behavior for the LQ models which induce destructive interference with standard γ exchange. For scalar LQs this happens for $\tilde{S}_1$, $R_{2\mathrm{R}}$ and $R_{2\mathrm{L}}$ (see Appendix). At HERA the window for LQ discovery falls essentially in the real domain. At the TESLA×HERA facility, however, this distinction between real or virtual LQ exchange will be mandatory.

In the following we will consider only the LQs in the real domain, at HERA.

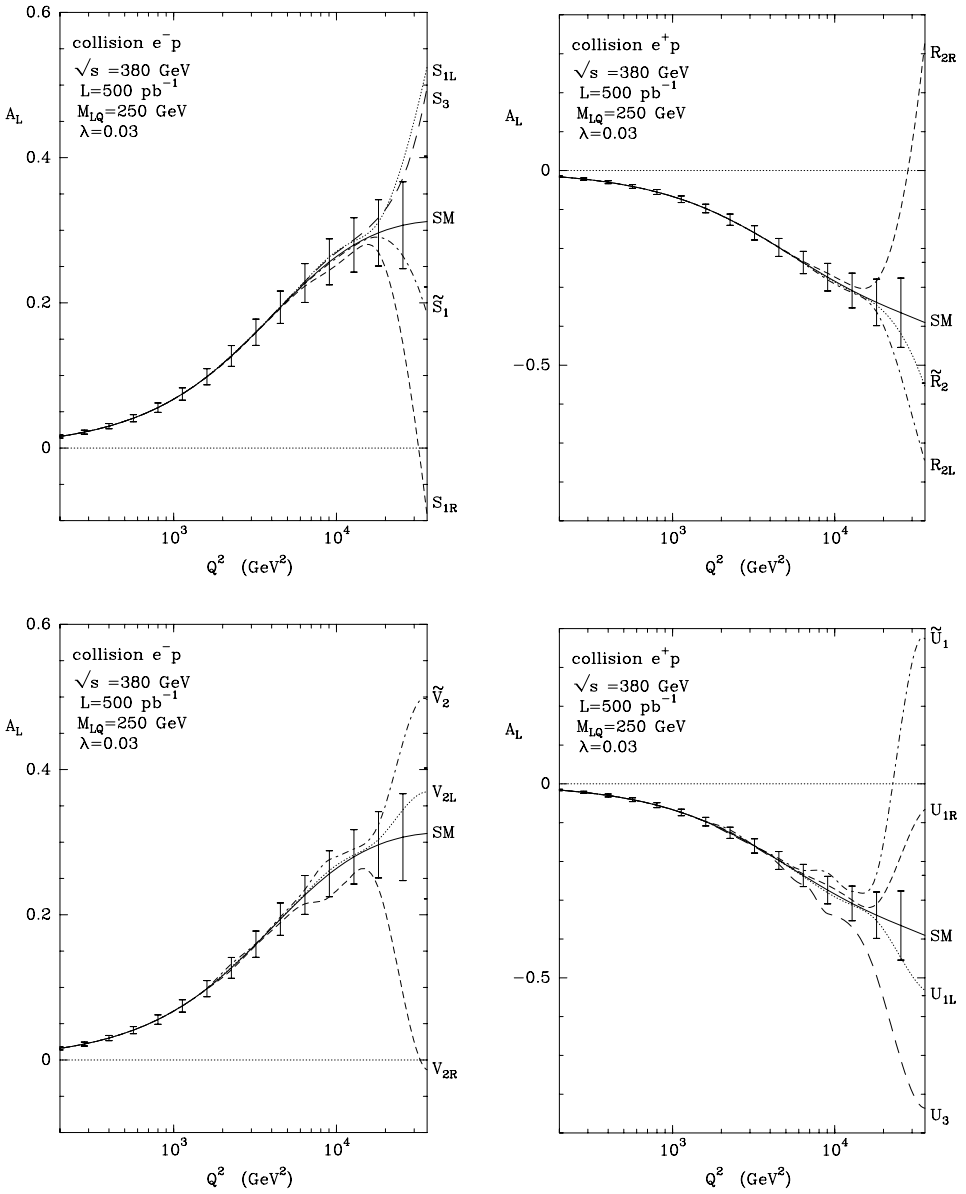

Fig. 4. $A_{\rm L}$ vs. Q^2 for the BRW models

Table 2. "Deviation signatures" for the BRW scalar LQ models (real domain)

	$S_{1\rm L}$	$S_{1\rm R}$	$\tilde{S}_1$	S_3	$R_{2\rm L}$	$R_{2\rm R}$	$\tilde{R}_2$
$A_{\rm L}(e^-)$	+	−	−	+	0	0	0
$A_{\rm L}(e^+)$	0	0	0	0	−	+	−
$A_{\rm LL}^{\rm PC}$	+	+	−	−	+	0	−

Therefore, adding the information which should be obtained from $A_{\rm L}(e^-p)$ (or from $A_{\rm LL}^{\rm PV}(e^-p)$), we now get a non-ambiguous separation of the LQ scalar models. This is shown by the different "deviation signatures" for all the different models presented in Table 2.

In this table, "0 deviation" means that the effect of a LQ on a particular quantity is contained into the error bar centered on the SM expectation. On the other hand, positive and negative deviations should be clearly visible thanks to the high integrated luminosities.

Vector case

Concerning vector LQs, the most sensitive quantities allowing the flavor separation are the polarized charge asymmetries. In the real domain the relevant charge asymmetries are B_U and B_V. These asymmetries are shown in Fig. 6. We have separated the effects of the classes ($U_{1\rm L}$,U_3) and ($U_{1\rm R}$,$\tilde{U}_1$) on B_U since these two classes are already distinguished thanks to the PV asymmetries.

The deviation signatures for vector LQs are displayed in Table 3.

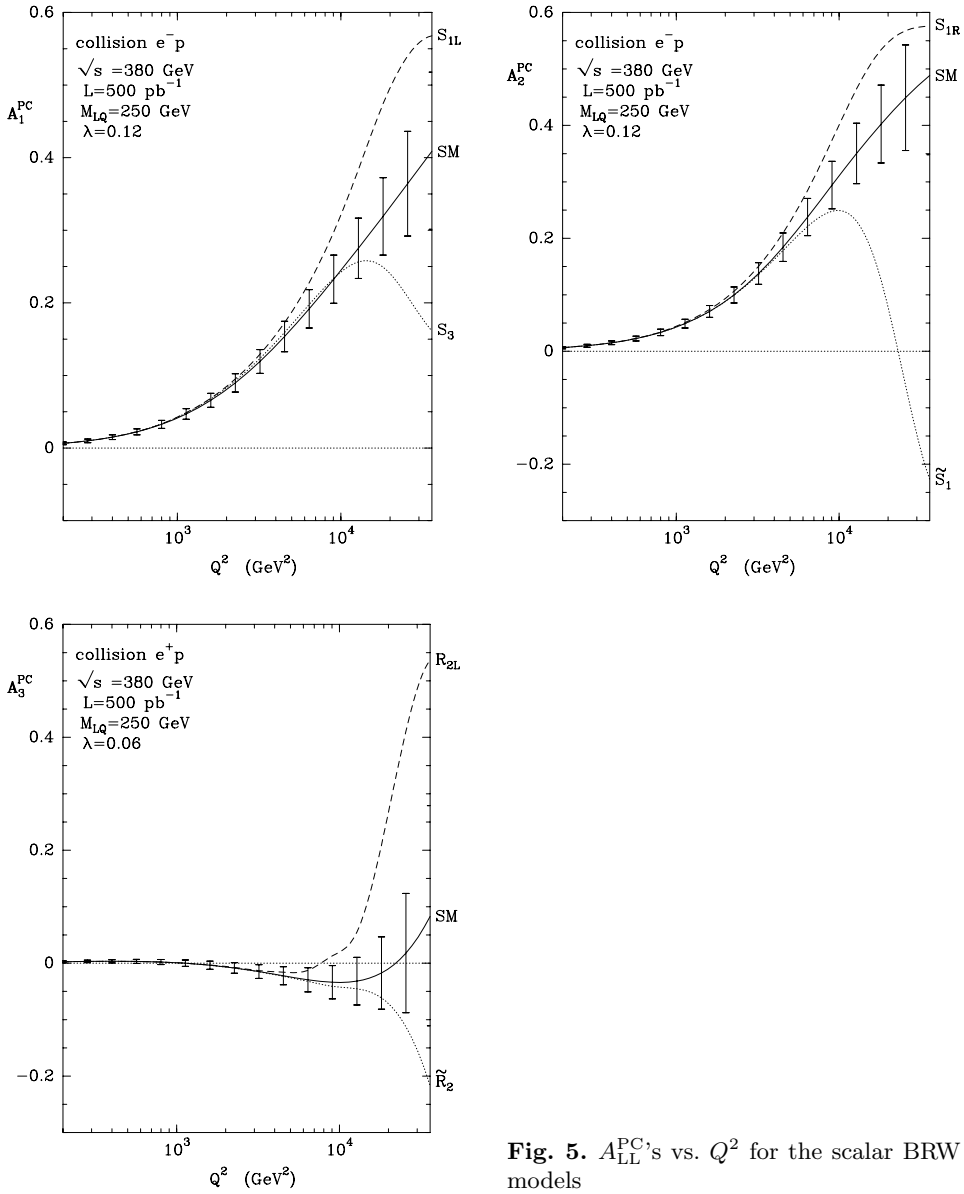

Fig. 5. $A_{\rm LL}^{\rm PC}$'s vs. Q^2 for the scalar BRW models

Table 3. "Deviation signatures" for the BRW vector LQ models (real domain)

	$U_{1\rm L}$	$U_{1\rm R}$	$\tilde{U}_1$	U_3	$V_{2\rm L}$	$V_{2\rm R}$	$\tilde{V}_2$
$A_{\rm L}(e^-)$	$-$	$+$	$+$	$-$	0	0	0
$A_{\rm L}(e^+)$	0	0	0	0	$+$	$-$	$+$
$B_{U\,\text{or}\,V}$	$+$	$-$	$+$	$-$	$+$	0	$-$

3.4 Identification domains

Finally, it is possible to estimate the domains in the (M, λ) plane where a non-ambiguous identification of the nature of a LQ should be possible. In Fig. 7 we present these "identification domains" for some representative examples.

The upper curves correspond to the present discovery limits from Tevatron, HERA and LEP. Constraints from APV have been omitted. The lower curves represent the constraints coming from the PV spin asymmetries. They are better, in general, than the ones from the PC or charge asymmetries (dashed curves). Note that, for $\tilde{V}_2$, the sensitivities from both types of asymmetries are equivalent.

The regions in the parameter space where a complete identification of the chiral structure is possible are given by the domains I+II. In domain I no effect will appear on the $A^{\rm PC}$'s nor B's and one misses the flavor separation. In the domain II it is possible to identify the nature of the LQ without ambiguity.

4 Conclusion

Concerning the chances of discovery of leptoquark states in the future HERA program (with a high integrated luminosity), we have seen that there are still some windows

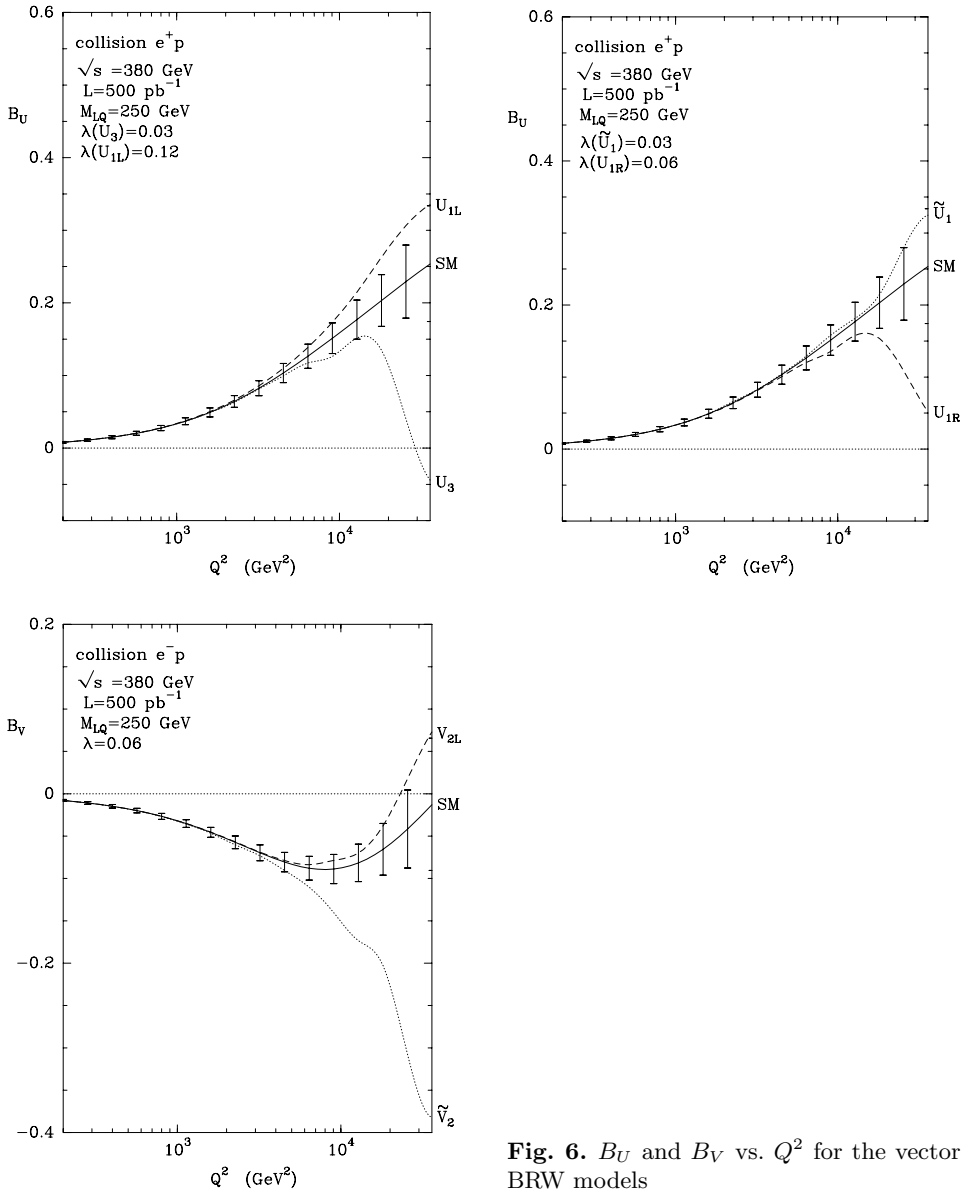

Fig. 6. B_U and B_V vs. Q^2 for the vector BRW models

that are not covered by present data, in particular in the real domain ($M < s^{1/2}$). Measurements of the integrated unpolarized cross section in NC processes, at the highest possible energy, should present the best opportunity. At this stage, polarized beams would not yield better results.

Our purpose was mainly to explore the possibilities of disentangling the various LQ models. We present in Fig. 8 a schematic view of what can be done from the precise measurements of the various observables we have discussed. The first two steps are well known: with unpolarized e^- and e^+ beams it is easy to get in the same time the separation between scalars and vectors (from the y distributions) and between $F = 0$ and $F = 2$ LQs (from $\mathrm{d}\sigma_\pm/\mathrm{d}Q^2$).

The next steps are more difficult to perform. However, it is mandatory to try to pin down the chiral structure of a newly discovered LQ-like particle. For example it is worth recalling here that, due to SUSY, the R-parity breaking squarks have universal left-handed couplings to leptons.

We have shown that polarization of the lepton beam should yield this information thanks to the precise measurement of A_L in both e^- and e^+ collisions. At this step the polarization of the proton beams is not necessary. Note also that the sensitivities of the PV asymmetry and of the unpolarized cross sections are comparable. This means that if polarized lepton beams are available in the same run, as soon as a LQ is discovered in e^+ or e^- collisions (via $\mathrm{d}\sigma/\mathrm{d}Q^2$) one gets almost simultaneously his scalar or vector nature (via $\mathrm{d}\sigma/\mathrm{d}y$) and the chiral structure of its couplings (via A_L).

Now, the next step is to try to get the flavor separation within the remaining classes of models, which is the most difficult task. Indeed, CC processes with unpolarized beams do not seem to be sufficient to fulfil this program, as long as "neutron" beams, through the use of ionized

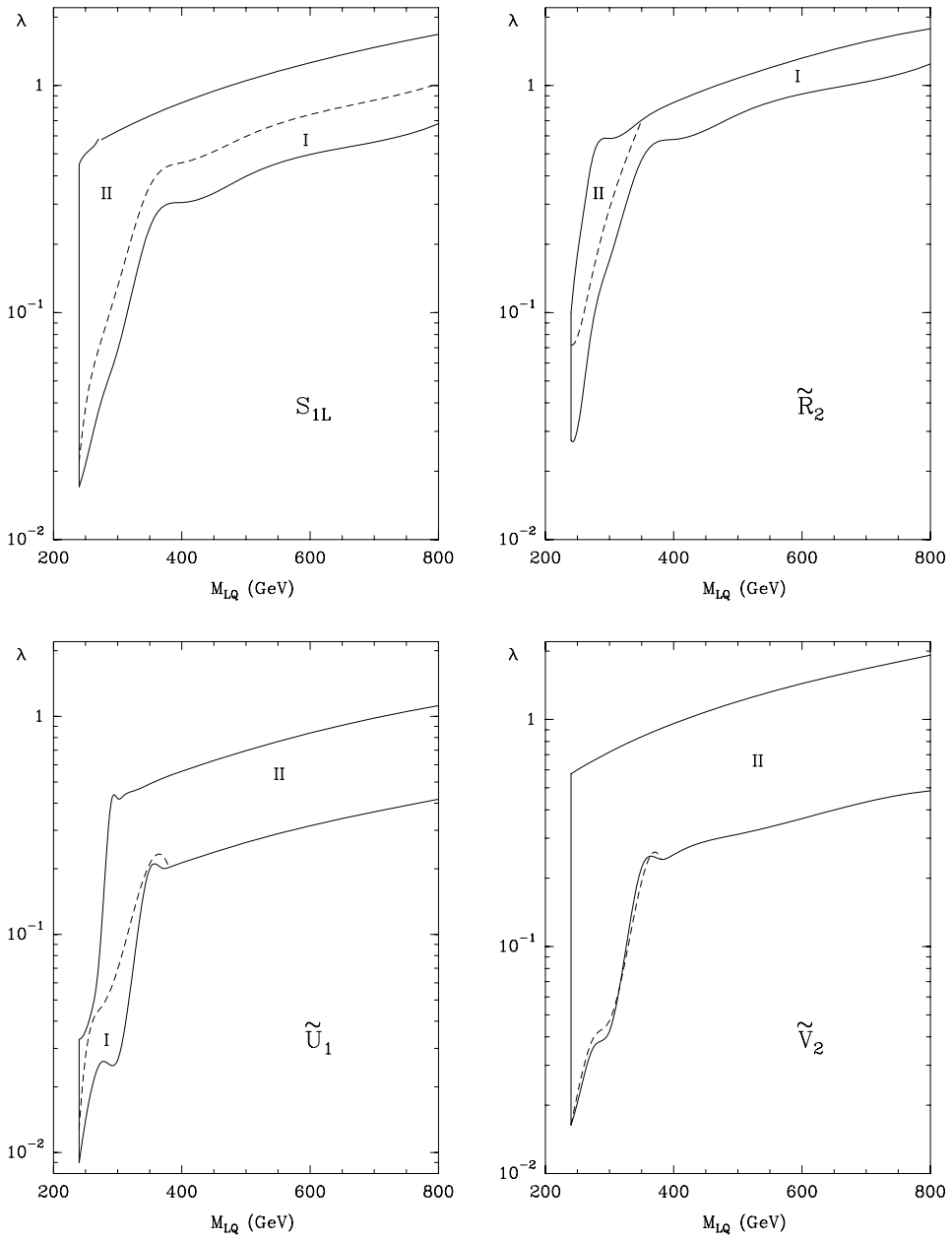

Fig. 7. Identification domain at 95% CL for S_{1L}, $\tilde{R}_2$, $\tilde{U}_1$ and $\tilde{V}_2$

deuterium or ^{3}He atoms, are not available. On the other hand, the behaviors of the polarized valence quark distributions Δu and Δd in a polarized proton should allow one to do this job. In the case of scalar LQs, measuring the PC double spin asymmetries is sufficient. In the case of the remaining vectors, it is necessary to measure some polarized charge asymmetries to obtain the separation at the same level of sensitivity. In both cases, the price to pay is a proton beam with a high degree of polarization ($P = 70\%$).

We feel that it was important to get an answer to the following question: are both (lepton and proton) polarizations mandatory to completely disentangle the various LQ models present in the BRW lagrangians? According to our analysis the answer is yes. This conclusion holds certainly also for the TESLA×HERA project.

Finally, if we relax the working assumptions (i)–(iv) (see Sect. 1), the LQs can have a more complex structure and the analysis should be less easy. In this case, like in the more general context of contact interactions [35], the use of additional asymmetries, that one can also define with lepton plus proton polarizations, should be very useful.

Moreover, polarized electron–neutron collisions could be performed with polarized ^{3}He beams: this option has been seriously considered in the framework of the RHIC-Spin program at Brookhaven and also at HERA [22]. This could be the final goal of an ambitious polarization program at HERA.

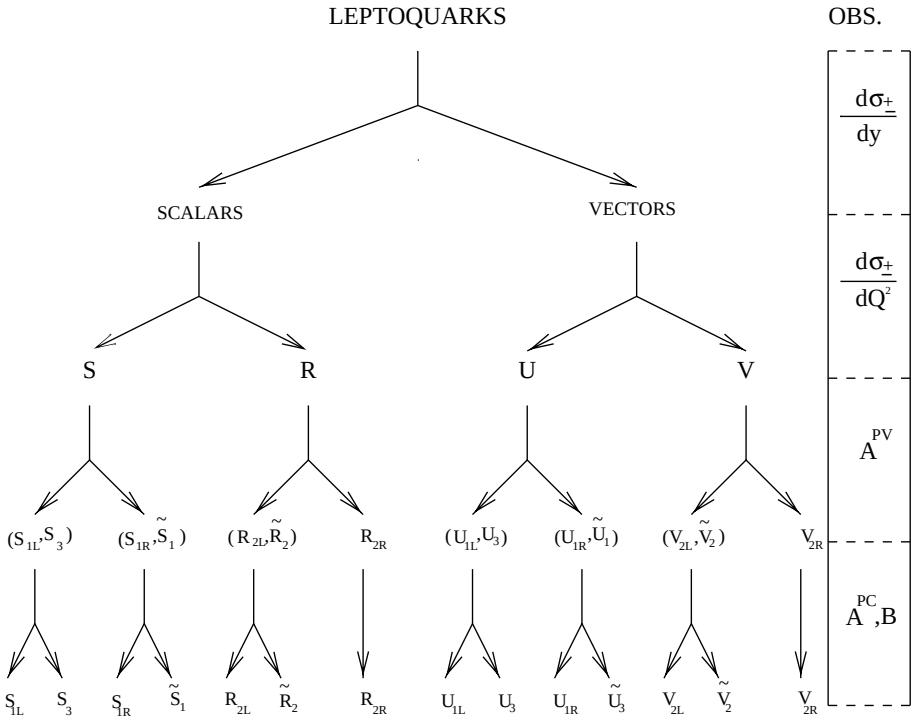

Fig. 8. Schematic view for LQ identification

Acknowledgements. We are indebted to A. De Roeck, J. Kalinowski, E. Reya, Y. Sirois, J. Soffer and W. Vogelsang for many interesting discussions and much information. JMV has the pleasure to thank the theoreticians of the "Institut für Physik" in Dortmund for helpful conversations and the excellent atmosphere, and finally, Susanne Laurent for her kindness and efficiency. The Alexander von Humboldt foundation is acknowledged for financial support.

A Appendix: cross sections

We present in this appendix the set of formulas necessary to calculate the double polarized cross sections, the spin and charge asymmetries involved in the present analysis.

A.1 Neutral current

Process

The single polarized cross sections are given in [4,3]. Here we give the cross sections in the (s, t, u) notation.

The collisions between charged leptons and protons in the neutral current channel correspond to the process $\vec{e}^{\pm}\vec{p} \longrightarrow e^{\pm}X$, whose cross section is given by

$$\frac{\mathrm{d}\sigma_t}{\mathrm{d}x\mathrm{d}Q^2}^{h_e h_p} = \sum_{h_q} \frac{\mathrm{d}\hat{\sigma}_t}{\mathrm{d}\hat{t}}^{h_e h_q} q_{h_p}^{h_q}(x,Q^2), \qquad \text{(A.1)}$$

where h_e, h_p and h_q are the helicities of the charged lepton, proton and parton (quark or antiquark), respectively. The label $t = \pm$ corresponds to the electric charge of the colliding lepton. $\sum_q$ represent the sum over all quark and antiquark flavors present inside the proton. The subprocess invariants $\hat{s}$, $\hat{t}$ and $\hat{u}$ are given by

$$\hat{s} = xs, \qquad \text{(A.2)}$$

$$\hat{t} = -Q^2, \qquad \text{(A.3)}$$

$$\hat{u} = xu = -x(1-y)s, \qquad \text{(A.4)}$$

where as usual the variable y is defined by $y = Q^2/xs$. We denote by $q_{h_p}^{h_q}(x,Q^2)$ the parton distribution for the parton q inside a proton of helicity h_p, with momentum fraction x and helicity h_q, at the energy scale Q^2. These distributions are related to the parallel and anti-parallel distributions by $q_+ = q_+^+ = q_-^-, q_- = q_+^- = q_-^+$, which are related to the usual unpolarized and polarized parton distributions by $q = q_+ + q_-$ and $\Delta q = q_+ - q_-$.

Subprocesses

Using the notation of [39], the cross section of the elementary subprocess $\vec{e}\vec{q} \to eq$ is given by

$$\frac{\mathrm{d}\hat{\sigma}_t}{\mathrm{d}\hat{t}}^{h_e h_q} = \frac{\pi}{\hat{s}^2} \sum_{\alpha,\beta} T_{\alpha,\beta}^{h_e h_q}(e^t,q), \qquad \text{(A.5)}$$

where $T_{\alpha,\beta}^{h_e h_q}(e^t,q)$ is the squared matrix element for α and β boson exchange. q is a quark or an antiquark. The $T_{\alpha,\beta}^{h_e h_q}(e^t,q)$ for the SM (i.e. for $\alpha,\beta = \gamma, Z$) are given in [35]. The $T_{\alpha,\beta}^{h_e h_q}(e^t,q)$ for LQ production, exchange and interferences with γ or Z, are given below. We have omitted the hat symbol of the variables $\hat{s}$, $\hat{t}$ and $\hat{u}$, for clarity.

Subprocess $e^- q \longrightarrow e^- q$

We have

$$T_{SS} = F^2 \frac{1}{64\pi^2} \frac{s^2}{s_S^2 + M_S^2 \Gamma_S^2} \times \left[\lambda_{\rm L}^4 (1-h_e)(1-h_q) + \lambda_{\rm R}^4 (1+h_e)(1+h_q)\right], \quad \text{(A.6)}$$

$$T_{VV} = F^2 \frac{1}{16\pi^2} \frac{u^2}{s_V^2 + M_V^2 \Gamma_V^2} \times \left[\lambda_{\rm L}^4 (1-h_e)(1+h_q) + \lambda_{\rm R}^4 (1+h_e)(1-h_q)\right], \quad \text{(A.7)}$$

$$T_{RR} = F^2 \frac{1}{64\pi^2} \frac{u^2}{u_{\rm R}^2} \times \left[\lambda_{\rm L}^4 (1-h_e)(1+h_q) + \lambda_{\rm R}^4 (1+h_e)(1-h_q)\right], \quad \text{(A.8)}$$

$$T_{UU} = F^2 \frac{1}{16\pi^2} \frac{s^2}{u_U^2} \times \left[\lambda_{\rm L}^4 (1-h_e)(1-h_q) + \lambda_{\rm R}^4 (1+h_e)(1+h_q)\right], \quad \text{(A.9)}$$

$$T_{\gamma S} = -F \frac{\alpha Q_e Q_q}{4\pi t} \frac{s^2 s_S}{s_S^2 + M_S^2 \Gamma_S^2} \times \left[\lambda_{\rm L}^2 (1-h_e)(1-h_q) + \lambda_{\rm R}^2 (1+h_e)(1+h_q)\right], \quad \text{(A.10)}$$

$$T_{\gamma V} = -F \frac{\alpha Q_e Q_q}{2\pi t} \frac{u^2 s_V}{s_V^2 + M_V^2 \Gamma_V^2} \times \left[\lambda_{\rm L}^2 (1-h_e)(1+h_q) + \lambda_{\rm R}^2 (1+h_e)(1-h_q)\right], \quad \text{(A.11)}$$

$$T_{\gamma R} = F \frac{\alpha Q_e Q_q}{4\pi t} \frac{u^2}{u_{\rm R}} \times \left[\lambda_{\rm L}^2 (1-h_e)(1+h_q) + \lambda_{\rm R}^2 (1+h_e)(1-h_q)\right], \quad \text{(A.12)}$$

$$T_{\gamma U} = F \frac{\alpha Q_e Q_q}{2\pi t} \frac{s^2}{u_U} \times \left[\lambda_{\rm L}^2 (1-h_e)(1-h_q) + \lambda_{\rm R}^2 (1+h_e)(1+h_q)\right], \quad \text{(A.13)}$$

$$T_{ZS} = -F \frac{\alpha_Z}{4\pi t_Z} \frac{s^2 s_S}{s_S^2 + M_S^2 \Gamma_S^2} \times [\lambda_{\rm L}^2 C_{eL} C_{qL} (1-h_e)(1-h_q) + \lambda_{\rm R}^2 C_{eR} C_{qR} (1+h_e)(1+h_q)], \quad \text{(A.14)}$$

$$T_{ZV} = -F \frac{\alpha_Z}{2\pi t_Z} \frac{u^2 s_V}{s_V^2 + M_V^2 \Gamma_V^2} \times [\lambda_{\rm L}^2 C_{eL} C_{qR} (1-h_e)(1+h_q) + \lambda_{\rm R}^2 C_{eR} C_{qL} (1+h_e)(1-h_q)], \quad \text{(A.15)}$$

$$T_{ZR} = F \frac{\alpha_Z}{4\pi t_Z} \frac{u^2}{u_{\rm R}} \times [\lambda_{\rm L}^2 C_{eL} C_{qR} (1-h_e)(1+h_q) + \lambda_{\rm R}^2 C_{eR} C_{qL} (1+h_e)(1-h_q)], \quad \text{(A.16)}$$

$$T_{ZU} = F \frac{\alpha_Z}{2\pi t_Z} \frac{s^2}{u_U} \times [\lambda_{\rm L}^2 C_{eL} C_{qL} (1-h_e)(1-h_q) + \lambda_{\rm R}^2 C_{eR} C_{qR} (1+h_e)(1+h_q)], \quad \text{(A.17)}$$

where α is the electromagnetic coupling, and $\alpha_Z = \alpha/\sin^2\theta_{\rm W}\cos^2\theta_{\rm W}$, $t_Z = t - M_Z^2$. $C_{f\rm L}$ and $C_{f\rm R}$ are the usual left-handed and right-handed couplings of the Z to the fermion f, given by $C_{f\rm L} = I_3^f - e_f \sin^2\theta_{\rm W}$, $C_{f\rm R} = -e_f \sin^2\theta_{\rm W}$ with $I_3^f = \pm 1/2$. For LQs, $s_{LQ} = s - M_{LQ}^2$ and $u_{LQ} = u - M_{LQ}^2$. The values for $\lambda_{\rm L}^2$, $\lambda_{\rm R}^2$ and the factor F are given in Table 4 for scalar LQs and in Table 5 for vector LQs. The factor F, given in term of combinations of Kronecker products, is relevant only when we convolute subprocess cross sections with pdfs.

Table 4. Parameters for the BRW scalar LQ models

	$S_{1\rm L}$	$S_{1\rm R}$	$\tilde{S}_1$	S_3	$R_{2\rm L}$	$R_{2\rm R}$	$\tilde{R}_2$
$\lambda_{\rm L}^2$	λ^2	0	0	λ^2	λ^2	0	λ^2
$\lambda_{\rm R}^2$	0	λ^2	λ^2	0	0	λ^2	0
F	δ_{qu}	δ_{qu}	δ_{qd}	$\delta_{qu} + 2\delta_{qd}$	δ_{qu}	$\delta_{qu} + \delta_{qd}$	δ_{qd}
$\lambda_{eq}.\lambda_{\nu q'}$	$-\lambda^2$	0	0	$+\lambda^2$	0	0	0

Table 5. Parameters for the BRW vector LQ models

	$U_{1\rm L}$	$U_{1\rm R}$	$\tilde{U}_1$	U_3	$V_{2\rm L}$	$V_{2\rm R}$	$\tilde{V}_2$
$\lambda_{\rm L}^2$	λ^2	0	0	λ^2	λ^2	0	λ^2
$\lambda_{\rm R}^2$	0	λ^2	λ^2	0	0	λ^2	0
F	δ_{qd}	δ_{qd}	δ_{qu}	$2\delta_{qu} + \delta_{qd}$	δ_{qd}	$\delta_{qu} + \delta_{qd}$	δ_{qu}
$\lambda_{eq}.\lambda_{\nu q'}$	$+\lambda^2$	0	0	$-\lambda^2$	0	0	0

Subprocess $e^+ q \longrightarrow e^+ q$

The squared matrix elements $T_{\alpha,\beta}$ are obtained from the twelve preceding equations with the following changes: $h_e \longleftrightarrow -h_e$, $s \longleftrightarrow u$, $1/(s_{LQ}^2 + M_{LQ}^2\Gamma_{LQ}^2) \longleftrightarrow 1/u_{LQ}^2$ and $s_{LQ}/(s_{LQ}^2 + M_{LQ}^2\Gamma_{LQ}^2) \longleftrightarrow 1/u_{LQ}$.

Subprocess $e^\pm \bar{q} \longrightarrow e^\pm \bar{q}$

The $T_{\alpha,\beta}$ are obtained from the ones for $e^\mp q$ scattering after the same transformations as above plus $h_q \longleftrightarrow -h_q$.

A.2 Charged current

The process for CC is $\vec{e^\pm}\vec{p} \longrightarrow \nu(\bar{\nu})X$ All the preceding formulas hold for CC processes with the following substitutions: $Q_{e,q} \to 0$, $C_{\rm L} \to 1$, $C_{\rm R} \to 0$, $\alpha_Z \to \alpha_W = \alpha_Z \cos^2\theta_{\rm W}$, $M_Z \to M_W$ and $t_Z \to t_W$. Concerning factor F, we have $F = \delta_{qu}(\delta_{qd})$ for $S_{1\rm L}$ and S_3 ($U_{1\rm L}$ and U_3). Finally, for $W \cdot LQ$ interferences one has now two different vertices in the diagram for LQ exchange (i.e. $e \cdot q \cdot LQ + \nu \cdot q' \cdot LQ$ vertices). Then the squared coupling $\lambda^2 \equiv \lambda_{eq}^2$ appearing in NC is changed to the product $\lambda_{eq}\lambda_{\nu q'}$. From (1) and (2) or from Table 1 of [3] we have $\lambda_{eq} = \pm\lambda_{\nu q'} = \pm\lambda$. The product $\lambda_{eq}\lambda_{\nu q'}$ is given in the last row of Tables 4 and 5.

References

1. P. Fayet, Phys. Lett. B **69**, 489 (1977); G. Farrar, P. Fayet, Phys. Lett. B **76**, 575 (1978)
2. Report of the $R_{\rm parity}$ group of the CNRS-GDR SUSY Working group, hep-ph/9810232
3. J. Kalinowski et al., Zeitschr. Phys. C **74**, 595 (1997)
4. W. Buchmüller, R. Rückl, D. Wyler, Phys. Lett. B **191**, 442 (1987)
5. S. Davidson et al., Zeitschr. Phys. C **61**, 613 (1994)
6. M. Leurer, Phys. Rev. D **50**, 536 (1994); Phys. Rev. D **49**, 333 (1994)
7. J. Hewett, T. Rizzo, Phys. Rev. D **56**, 5709 (1997); Phys. Rev. D **58**, 055005 (1998); A. Deandrea, Phys. Lett. B **409**, 277 (1997)
8. Leptoquark Limit Combination Working Group, hep-ex/9810015
9. J. Blümlein et al., Zeitschr. Phys. C **76**, 137 (1997); hep-ph/9811271; and references therein
10. D0 Collaboration, ICHEP98, Vancouver, Canada; http://www-d0.fnal.gov/public/new/new_public.html #conferences
11. S.C. Bennett, C.E. Wieman, Phys. Rev. Lett. **82**, 2484 (1999)
12. Particle Data Group, Eur. Phys. J. C **3**, 1 (1998)
13. R. Casalbuoni et al., Phys. Lett. B **460**, 135 (1999)
14. V. Barger et al., Phys. Rev. D **57**, 3833 (1998)
15. K. Ackerstoff et al., OPAL Collaboration, Eur. Phys. J. C **2**, 441 (1998)
16. H1 Collaboration, hep-ex/9907002 submitted to Eur. Phys. J. C; T. Matsushita, E. Perez, R. Rückl, in [23]; J. Phys. G **25**, 1418 (1999)
17. J.-M. Virey, E. Tuğcu, P. Taxil, in Proceedings of the 7th Workshop on Deep Inelastic Scattering and QCD, DESY-Zeuthen, Germany, April 1999, Nucl. Phys. B (Proc. Suppl.) **79**, 617 (1999); P. Taxil et al., in [24]
18. M. Botje, G. Wolf, DESY 98-140, hep-ex/9809027
19. Y. Sirois, in Proceedings of the 7th Workshop on Deep Inelastic Scattering and QCD, DESY-Zeuthen, Germany, April 1999
20. RHIC Spin Collaboration, Letter of intent, April 1991; G. Bunce et al., Polarized protons at RHIC, Particle World **3**, 1 (1992); Proceedings of the RSC annual meeting, Marseille, September 1996, preprint CPT-96/P.3400; Proceedings of RIKEN-BNL Research Center Workshop, RHIC Spin Physics, April 1998, preprint BNL-65615
21. 1996 HERA Workshop, Future Physics at HERA, edited by G. Ingelman, A. De Roeck, R. Klanner
22. 1997 Workshop on Physics with Polarized Protons at HERA, edited by A. De Roeck, T. Gehrmann; desy-proceedings-1998-01
23. 3$^{\rm rd}$ UK Phenomenology Workshop on HERA Physics, Durham, UK, September 1998, edited by R. Devenish et al.; J. Phys. G **25**, 1269 (1999)
24. Workshop on Polarized Protons at High Energies - Accelerator Challenges, Physics Opportunities, DESY-Hamburg, Germany, May 1999, edited by D. Barber et al.
25. M. Glück, E. Reya, A. Vogt, Zeitschr. Phys. C **67**, 433 (1995)
26. T. Plehn, H. Spiesberger, M. Spira, P.M. Zerwas, Zeitschr. Phys. C **74**, 611 (1997)
27. Z. Kunszt, W.J. Stirling, Zeitschr. Phys. C **75**, 453 (1997)
28. M.A. Doncheski, J.L. Hewett, Zeitschr. Phys. C **56**, 209 (1992)
29. G. Altarelli, Nucl. Phys. Proc. Suppl. **62**, 3 (1998) and references therein
30. R.D. Ball et al., p. 777 of [21]; A. De Roeck et al., Eur. Phys. J. C **6**, 121 (1999)
31. A. De Roeck, private communication
32. M. Glück, E. Reya, M. Stratmann, W. Vogelsang, Phys. Rev. D **53**, 4775 (1996)
33. C. Bourrely et al., Phys. Rep. **177**, 319 (1989); J. Soffer, J.-M. Virey, Nucl. Phys. B **509**, 297 (1998)
34. B. Lampe, E. Reya, hep-ph/9810270, to appear in Phys. Rep
35. J.-M. Virey, Eur. Phys. J. C **8**, 283 (1999)
36. K.S. Babu et al., Phys. Lett. B **408**, 261 (1997)
37. Y. Sirois, private communication
38. P. Taxil, J.-M. Virey, Phys. Lett. B **441**, 376 (1998) and references therein
39. C. Bourrely, J. Ph. Guillet, J. Soffer Nucl. Phys. B **361**, 72 (1991)